

# Laser Cooling in Semiconductor Heterojunctions by Extraction of Photogenerated Carriers

Paul Dalla Valle<sup>1</sup>, Marc Bescond,<sup>1,2</sup> Fabienne Michelini<sup>1</sup>, and Nicolas Cavassilas<sup>1,\*</sup>

<sup>1</sup>*Aix Marseille Université, CNRS, Université de Toulon, IM2NP UMR 7334, 13397 Marseille, France*

<sup>2</sup>*Institute of Industrial Science, University of Tokyo, 4-6-1 Komaba Meguro-ku, Tokyo, 153-8505, Japan*



(Received 23 March 2023; revised 7 July 2023; accepted 11 July 2023; published 31 July 2023)

Laser cooling of a semiconductor material, in which heat is extracted by the emission of photons, requires near-perfect external radiative efficiency. In this theoretical work, we propose a cooling system based on carrier extraction in a large-band-gap reservoir. The electron-hole pairs generated in the material to be cooled are extracted in such a reservoir by absorption of phonons, then carrying a heat flux. With an analytical detailed-balance model, we show that this concept is applicable even in materials with moderate external radiative efficiency. Moreover, by adjustment of the band gap of the reservoir to the laser power, this system can either reach high efficiency or transfer high power with lower efficiency.

DOI: 10.1103/PhysRevApplied.20.014066

## I. INTRODUCTION

Optical refrigeration of solids, originally proposed in 1929, is based on anti-Stokes fluorescence, where the extracted photoluminescent energy exceeds the energy of the incident photons. This up-conversion process is induced by the absorption of thermal energy from the system, leading to its cooling [1]. Epstein *et al.* [2] reported in 1995 the first experimental evidence of laser-induced refrigeration in a Yb<sup>3+</sup>-doped glass. Since then, many advances in the field of rare-earth-doped solids have been reported and reviewed [3,4]. Besides, great interest has grown for optical refrigeration of semiconductors to enhance the performance of many optoelectronic devices [5]. The refrigeration of semiconductor materials with a laser requires a laser energy very close to the band gap or even lower [6]. On the basis of the Sheik-Bahae–Epstein theory [7], the net laser cooling of a semiconductor can occur in three different ways: possessing a large energy difference between the mean photoemission and the incident photons, having an external radiative efficiency (ERE) close to unity, and having absorption efficiency near unity [8]. Laser cooling has been investigated in various semiconductors [3,4]. In II-VI materials, Zhang *et al.* [8] observed a cooling of 40 K in CdS nanobelts. Ha *et al.* [9] reported a net cooling directly from ambient temperature in lead halide perovskite due to a strong photoluminescence up-conversion and an ERE of 99.8%. A dominant anti-Stokes photoluminescence was reported in germanium nanocrystals, and a laser cooling of 50 K was inferred

[5]. In III-V semiconductors, even if up-conversion processes have been highlighted, no net cooling was observed because of residual below-band-gap absorption [10] or because the ERE was not sufficient [11,12]. Theoretical efforts were conducted to improve the optical refrigeration of semiconductors. Previous studies highlighted the importance of excitonic resonance [13] and photon recycling [14,15]. Coupled quantum wells [16] and band-gap engineering [17] were proposed to increase the net cooling efficiency.

In this theoretical work, we propose basing the cooling on the extraction of the carriers into a large-band-gap reservoir instead of on their recombination. From a detailed-balance model, we show that extraction-based laser cooling can be much more efficient than the cooling obtained from radiative recombination. Interestingly, this method works even with a modest ERE. For that, a type-I heterojunction, consisting of a small-band-gap absorber connected to a large-band-gap reservoir, can transport thermal energy from the absorber to the reservoir in the form of potential carrier energy. The laser must photogenerate carriers in the absorber with an energy lower than the band gap of the reservoir. Those carriers are extracted into the reservoir by absorbing phonons, leading to evaporative cooling in the absorber. By adjustment of the band offsets between the absorber and the reservoir, it will be possible to either have high efficiency at low power or higher power with lower efficiency. We note that our proposal is very general and the concept of extraction-based optical refrigeration should apply to any type-I heterojunction.

This article is organized as follows. We first describe the system and the approach used to model it. Then, by varying the system's architecture, we highlight the origin

\* nicolas.cavassilas@im2np.fr

of the cooling process. Finally, with realistic parameters, we show that this process leads to high cooling power, even with a modest ERE.

## II. MODEL

For clarity, before the simple type-I heterojunction, we consider the double heterojunction shown in Fig. 1. A semiconducting absorber, with band gap  $E_g$ , is set between two reservoirs. The left (right) reservoir creates a contact in the valence (conduction) band but offers an infinite barrier in the conduction (valence) band. When an electron-hole pair is generated in the absorber, apart from recombining, the electron (hole) can go only to the right (left) reservoir. This system then behaves like a solar cell [18]. We design the reservoirs in such a way that the energy difference between the valence-band maximum of the left reservoir and the conduction-band minimum of the right reservoir, denoted  $E_{cv}$ , is greater than  $E_g$ . An electron in the bottom of the conduction band of the absorber must absorb phonons to reach the right reservoir (the same for holes and the left reservoir). In our model, the reservoirs are of infinite size. Thus, they can accept or provide as many carriers as necessary, without modifying their electronic distribution, which remains at 300 K. Finally, the Fermi levels of these two reservoirs can be shifted by applying a bias  $V = \mu_R - \mu_L$ .

To model this system, we use a detailed-balance approach. In the absorber, we assume a generation rate of electron-hole pairs equal to the photon flux:

$$\begin{aligned} J_{\text{gen}} &= \int_{E_g}^{\infty} \phi_{\text{in}}(E) dE, \\ P_{\text{gen}} &= \int_{E_g}^{\infty} \phi_{\text{in}}(E) E dE, \end{aligned} \quad (1)$$

where  $J_{\text{gen}}$  is the photon flux and  $P_{\text{gen}}$  is the corresponding power flux density. In the following, we use a boxcar function to simulate the laser spectrum  $\phi_{\text{in}}(E)$ .

Once electrons and holes have been generated, we assume that they thermalize instantaneously via carrier-carrier interactions [19]. Their distribution is then a Fermi function with a temperature and Fermi level that must be determined. We assume the same temperature  $T_c$  for electrons and holes, but different Fermi levels  $\mu_e$  and  $\mu_h$ , with  $\Delta\mu = \mu_e - \mu_h$ . In our model, we consider that the crystal lattice remains at  $T_{\text{amb}} = 300$  K, meaning that the phononic bath remains at 300 K. Therefore, if  $T_c$  is different from 300 K, the carriers and the phonons are not in equilibrium with each other. This implies an exchange of energy in the direction of equilibrium. Obtaining  $T_c > 300$  K means that the carriers emit phonons, and thus there is heat transfer from the electronic bath toward the phononic bath. In contrast, if  $T_c < 300$  K, there is absorption of phonons and thus heat transfer in the reverse direction. Recent experimental results [20], concerning

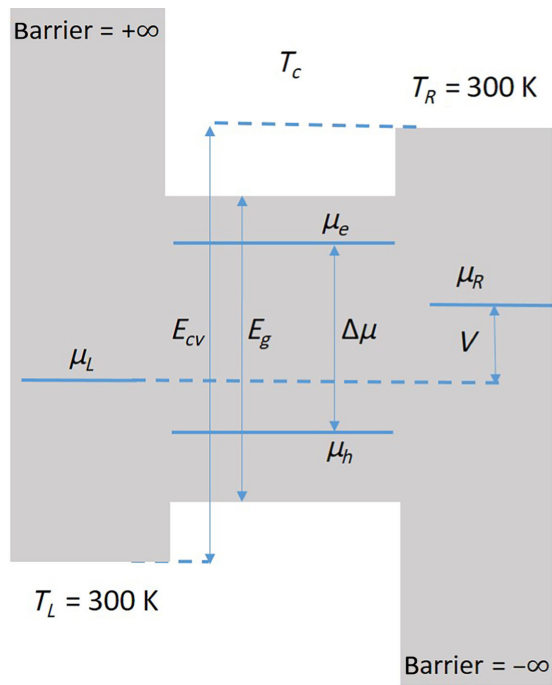


FIG. 1. The double heterojunction. This system is made of a small-band-gap absorber between two reservoirs. In the whole system, the phonon temperature is set to 300 K. We model not the cooling of the materials but only the heat fluxes. In the reservoirs, electrons are always considered at 300 K, and we apply a bias between the Fermi levels such that  $V = \mu_R - \mu_L$ . In our model, by solving the carrier and power-flux conservation equations, we calculate  $T_c$  and  $\Delta\mu = \mu_e - \mu_h$  for given  $E_g$ ,  $E_{cv}$ ,  $V$ , and illumination.

hot-carrier solar cells, show that the power exchanged with the phononic bath can be expressed as

$$P_{\text{phonon}}(T_c) = Q(T_c - T_{\text{amb}}), \quad (2)$$

where  $Q$  is a coefficient specific to each material and system (quantum well or bulk, for example). The higher the value of this parameter is, the more efficient the energy transfer between the electronic and phononic baths is. This offers a simple way to simulate the consequences of complex behaviors such as electron-optical-phonon interactions, electron-acoustic-phonon interactions, and acoustic-phonon-optical-phonon interactions. For bulk GaAs,  $Q = 2 \times 10^5 \text{ W m}^{-2} \text{ K}^{-1}$  for a thickness of 100 nm (which is sufficient to absorb the photon flux). First, we use this value for our implementations. Subsequently, by varying  $Q$  over several orders of magnitude, we show that this factor has very little effect on the cooling efficiency of our system. If  $T_c < T_{\text{amb}}$ , carriers in the absorber have consumed phonons, and then  $P_{\text{phonon}}$  is negative.

Once generated and thermalized, the carriers can recombine. To simulate this recombination, we follow the approach given by Tsai [19]. If the conditions  $E \gg$

$k_B T$  and  $(E - \Delta\mu) \gg k_B T$  are satisfied, we can express the electronic distribution using the Maxwell-Boltzmann approximation. Thus,

$$\begin{aligned} J_{\text{rec}}(\Delta\mu, T_c) &= \frac{1}{\eta_{\text{rad}}} \int_{E_g}^{\infty} \phi_{\text{BB}}(E) e^{\frac{\eta_c(T_c)E}{k_B T_{\text{amb}}}} e^{-\frac{(1-\eta_c(T_c))\Delta\mu}{k_B T_{\text{amb}}}} dE, \\ P_{\text{rec}}(\Delta\mu, T_c) &= \frac{1}{\eta_{\text{rad}}} \int_{E_g}^{\infty} E \phi_{\text{BB}}(E) e^{\frac{\eta_c(T_c)E}{k_B T_{\text{amb}}}} e^{-\frac{(1-\eta_c(T_c))\Delta\mu}{k_B T_{\text{amb}}}} dE, \end{aligned} \quad (3)$$

where

$$\phi_{\text{BB}}(E) = \frac{2\pi}{h^3 c^2} \times \frac{E^2}{\exp\left(\frac{E}{k_B T_{\text{amb}}}\right) - 1} \quad (4)$$

is the black-body radiation at room temperature  $T_{\text{amb}}$ , given by Plank's law,

$$\eta_c(T_c) = 1 - \frac{T_{\text{amb}}}{T_c} \quad (5)$$

is the Carnot efficiency,  $J_{\text{rec}}$  is the number of electron-hole pairs that recombine per unit of time and surface, and  $P_{\text{rec}}$  is the corresponding power flux density. The integral part of  $J_{\text{rec}}$  corresponds to the emission of a black body  $\phi_{\text{BB}}$  of temperature  $T_c$  [19]. We then have radiative recombination (emission of photons). To consider nonradiative recombination, we divide the radiative recombination by the ERE. In III-V materials and lead halide perovskites, when they are pure, the ERE is close to 1 [9,11]. On the other hand, in IV-IV materials with an indirect band gap, the ERE can be much lower and could reach values as low as  $10^{-4}$  [21].

Rather than recombining, the carriers can also be extracted into the reservoirs. We have a flux of carriers through the left and right contacts. Knowing that to conserve the total current these fluxes must be equal, we can write the current and the corresponding power as follows:

$$\begin{aligned} J_{\text{contact}}(\Delta\mu, T_c) &= \int_{E_{cv}}^{\infty} \frac{8\pi m^*}{h^3} (E - E_{cv}) \left( \frac{1}{1 + \exp\left(\frac{(1-\eta_c(T_c))(E-\Delta\mu)}{2k_B T_{\text{amb}}}\right)} - \frac{1}{1 + \exp\left(\frac{E-V}{2k_B T_{\text{amb}}}\right)} \right) dE, \\ P_{\text{contact}}(\Delta\mu, T_c) &= \int_{E_{cv}}^{\infty} \frac{8\pi m^*}{h^3} (E - E_{cv}) \left( \frac{1}{1 + \exp\left(\frac{(1-\eta_c(T_c))(E-\Delta\mu)}{2k_B T_{\text{amb}}}\right)} - \frac{1}{1 + \exp\left(\frac{E-V}{2k_B T_{\text{amb}}}\right)} \right) EdE. \end{aligned} \quad (6)$$

The derivation of these original expressions, presented in detail in the Appendix, is based on the Landauer approach, which supposes that the electronic distributions of the absorber and the reservoirs do not directly interact through carrier-carrier scattering. In the model shown in Fig. 1, by defining three electronic distributions (for the two reservoirs and the absorber), this assumption is implicit. The Landauer approach also introduces the notion of transmission, which is the probability for an electron to cross the interface without reflection. Here we assume that this probability is unity, as we consider only the case where the passage through the contact is perfect. This ignores the quantum reflection due to the passage from one material to another, and the possible scattering on the interface, which is assumed to be perfectly abrupt. Following a three-dimensional (3D) description of the Landauer approach,  $J_{\text{contact}}$  is given by the integration of the term  $[m^*(E - E_{cv})]$  times the difference between the Fermi functions in the absorber and the reservoir, where  $m^*$  is the effective mass in the reservoir and  $E$  is the total energy of the carriers. This term is derived from the 3D density of states in the reservoirs  $\rho_{3D} = 2m^*(E - E_{cv})/\hbar^2 \pi^2 dk/d(E - E_{cv})$ , multiplied by the velocity of the carriers  $v = 1/2\hbar d(E - E_{cv})/dk$ . As  $J_{\text{contact}}$  and  $P_{\text{contact}}$  are proportional to  $m^*$ , we use the

limiting (smallest) effective mass for the implementation. For III-V semiconductors, the smallest effective mass is the effective mass of the  $\Gamma$  valley of the conduction band.

Finally, to describe the carrier distribution in the absorber, we calculate  $T_c$  and  $\Delta\mu$  using the conservation of particles and power fluxes for a given bias  $V$  and a given reservoir band gap  $E_{cv}$ :

$$\begin{aligned} J_{\text{gen}} &= J_{\text{rec}}(\Delta\mu, T_c) + J_{\text{contact}}(\Delta\mu, T_c), \\ P_{\text{gen}} &= P_{\text{rec}}(\Delta\mu, T_c) + P_{\text{contact}}(\Delta\mu, T_c) + P_{\text{phonon}}(T_c). \end{aligned} \quad (7)$$

### III. RESULTS AND DISCUSSION

Figure 2 shows  $J_{\text{contact}}$ ,  $T_c$ , and  $\Delta\mu$  as a function of the bias  $V$  for  $E_g = 0.74$  eV,  $E_{cv} = E_g + 0.25$  eV,  $m^* = 0.08m_0$  (with  $m_0$  the free electron mass), and incident power  $P_{\text{gen}} = 800$  W cm $^{-2}$ . The laser generates photons with energy between  $E_g$  and  $E_g + 10$  meV. This system has the current-voltage characteristic of a solar cell with short-circuit current density  $J_{\text{SC}} = 1068$  A cm $^{-2}$  and open-circuit voltage  $V_{\text{OC}} = 0.655$  V. This is not surprising, since the system described in Fig. 1 is equivalent to a solar cell with the  $p$  ( $n$ ) contact on the left (right). When  $V = V_{\text{OC}}$ , we have  $T_c = 299$  K and  $\Delta\mu = 0.656$  V. These values are, respectively, very close to the temperature of the reservoirs

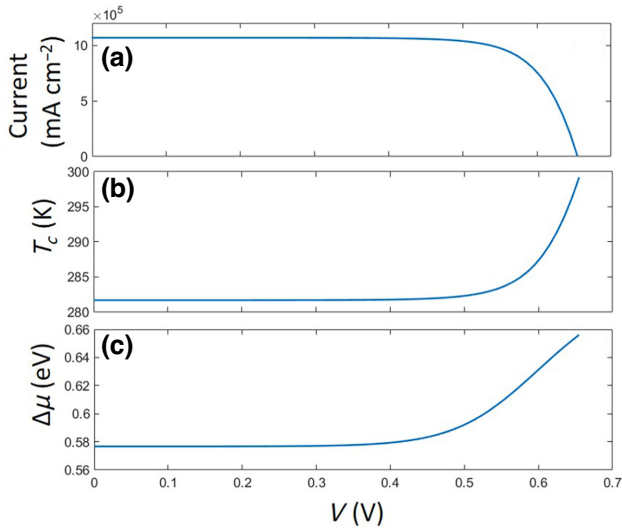


FIG. 2. (a) Charge current density  $q \times J_{\text{contact}}$ , (b) carrier temperature in the absorber  $T_c$ , and (c) Fermi+level splitting in the absorber  $\Delta\mu$  as a function of the bias  $V$  applied between the two reservoirs. Calculations are conducted for  $E_g = 0.47 \text{ eV}$ ,  $E_{cv} = 0.99 \text{ eV}$ ,  $\eta_{\text{rad}} = 10^{-2}$ , and an illumination power of  $800 \text{ W cm}^{-2}$  between  $E_g$  and  $E_g + 10 \text{ meV}$ .

(300 K) and the voltage  $V = 0.655 \text{ V}$ . The electrons (holes) in the absorber are almost in equilibrium with the electrons (holes) in the right (left) reservoir. At  $V = 0 \text{ V}$  we obtain  $T_c = 282 \text{ K}$  and  $\mu = 0.576 \text{ V}$ . The large value of the Fermi level splitting, compared to the applied voltage, indicates that we have an accumulation of cold carriers in the absorber that are no longer in equilibrium with the reservoirs.

To better understand the physical mechanism at  $V = 0 \text{ V}$ , we show in Fig. 3(a)  $T_c$  and in Fig. 3(b)  $J_{\text{contact}}/J_{\text{gen}}$  and  $J_{\text{rec}}/J_{\text{gen}}$  for different values of  $E_{cv} > E_g$  (with  $E_g$  constant). The laser power is fixed, meaning that  $J_{\text{gen}}$  and  $P_{\text{gen}}$  are constants. When  $E_{cv} = E_g$ , the carriers are easily extracted into the reservoirs ( $J_{\text{contact}}/J_{\text{gen}} = 1$ ) and  $T_c = 295 \text{ K}$ . On the other hand, when  $E_{cv}$  is large, the carriers are no longer extracted by the contacts ( $J_{\text{contact}}/J_{\text{gen}} = 0$ ) and are all recombined ( $J_{\text{rec}}/J_{\text{gen}} = 1$ ). We then find the behavior in Fig. 2(b) at  $V = V_{\text{OC}}$  (zero current and  $T_c = 299 \text{ K}$ ). Between these two extreme cases,  $T_c$  reaches a minimum. Starting from  $E_{cv} = E_g$ ,  $T_c$  decreases linearly with the increase of  $E_{cv}$ . Nevertheless, beyond a certain value of  $E_{cv}$ ,  $J_{\text{contact}}$  decreases and the temperature rises with increasing  $J_{\text{rec}}/J_{\text{gen}}$ . The carrier temperature is thus the result of a trade-off between the energy at which the carriers are extracted and the extraction flux. We are therefore dealing with an evaporative cooling, i.e., when the extraction of high-energy carriers cools the whole distribution [22]. This carrier cooling implies a thermal power flux from the phononic bath toward the electronic bath, given by  $-P_{\text{phonon}}$ . Another way to interpret this process

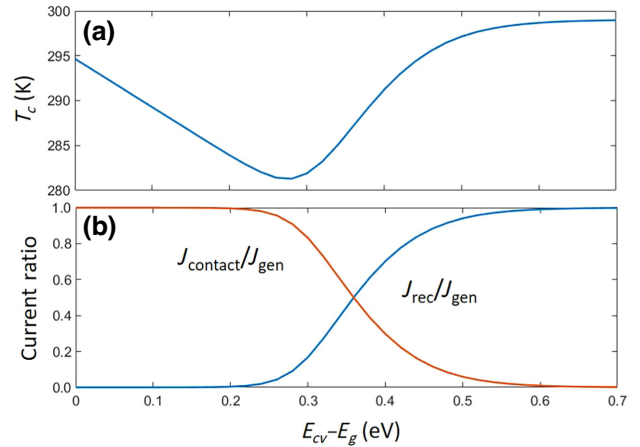


FIG. 3. For the same parameters as used to obtain the results shown in Fig. 2 (except for  $E_{cv}$ ), at  $V = 0 \text{ V}$ , (a)  $T_c$  and (b) the current ratios  $J_{\text{contact}}/J_{\text{gen}}$  and  $J_{\text{rec}}/J_{\text{gen}}$  are shown versus  $E_{cv} - E_g$ .

is that the carriers must absorb phonons to reach the contacts. The higher  $E_{cv}$  is, the more phonons are absorbed. Once the contact is reached, the carriers diffuse into the reservoir with this thermal energy as potential energy. If  $E_{cv}$  is too high, the carriers can no longer reach the contacts. In the case in Fig. 3, the best trade-off is obtained when  $E_{cv} = E_g + 0.28 \text{ eV}$ .

We now analyze the carrier temperatures, presented in Fig. 3, with large  $E_{cv}$  and  $E_{cv} = E_g$ . When  $E_{cv}$  is large, the contacts isolate the absorber from the reservoirs and we are in the classical case of radiative cooling with a single material. The carriers have a temperature lower than 300 K (299 K) because they are photogenerated with an average energy (5 meV) lower than thermal energy. When  $E_{cv} = E_g$ , we obtain  $T_c = 295 \text{ K}$ ; the fact that this temperature is lower (295 K against 299 K) shows that the heat extraction through contacts is more efficient than the heat extraction based on recombination.

From the analysis performed on the solar cell, we now propose designing a cooling system with a single reservoir, typically the type-I heterojunction schematically shown in Fig. 4. Here, electrons and holes photogenerated in the absorber evaporate in the same reservoir. Such a reservoir has to be thick enough to allow the recombination of all the carriers injected from the absorber with a reduced Fermi-level splitting. For an infinite reservoir in our model, all electrons and holes recombine and they share the same Fermi level  $\mu_{\text{res}}$  (equivalent to  $V = 0 \text{ V}$  in the system presented in Fig. 1). We define the cooling efficiency as the ratio between the cooling power in the absorber and the generation power imposed by the laser. The cooling power is the balance between the phonons consumed through  $P_{\text{phonon}}$  and the phonons emitted through nonradiative recombination in the absorber [i.e.,  $(1 - \eta_{\text{rad}})P_{\text{rec}}$ ].

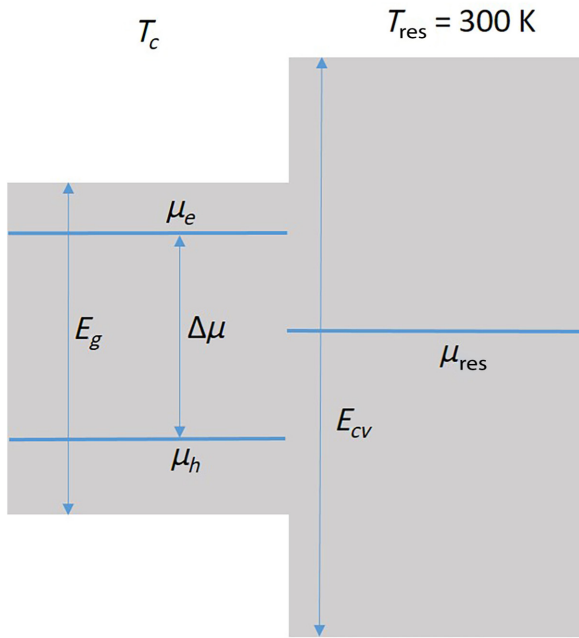


FIG. 4. The system with one reservoir. The reservoir being infinite, all carriers injected from the absorber can recombine in the reservoir without Fermi-level splitting between electrons and holes.

As  $P_{\text{phonon}}$  is negative when phonons are extracted [see Eq. (2)], the cooling efficiency is defined as

$$\eta_{\text{cooling}} = \frac{-P_{\text{phonon}} - (1 - \eta_{\text{rad}})P_{\text{rec}}}{P_{\text{gen}}} \quad (8)$$

The cooling efficiency  $\eta_{\text{cooling}}$  is positive (cooling of the absorber) if  $P_{\text{phonon}}$  is negative, with an absolute value greater than  $(1 - \eta_{\text{rad}})P_{\text{rec}}$ .

We explore the potentialities of an  $\text{In}_{0.53}\text{Ga}_{0.47}\text{As}/\text{InP}$  heterojunction as a cooling system controlled by a laser. We focus on this type-I heterojunction to give a concrete example, but there is no evidence that this heterojunction is better than any other heterojunction for refrigeration. Considering  $\text{In}_{0.53}\text{Ga}_{0.47}\text{As}$  for the absorber ( $E_g = 0.74$  eV) and InP for the infinite reservoir ( $E_{cv} = 1.34$  eV), we compute the cooling efficiency versus the laser power  $P_{\text{gen}}$ , shown Fig. 5. We do this calculation for  $\eta_{\text{rad}} = 1$  and  $\eta_{\text{rad}} = 10^{-2}$ . At low power, for both values of the  $\eta_{\text{rad}}$ , the process offers high efficiencies. With  $\eta_{\text{rad}} = 1$  ( $\eta_{\text{rad}} = 10^{-2}$ ), we obtain, for instance, an efficiency of 94% (82%) for  $P_{\text{gen}} = 80 \text{ mW cm}^{-2}$ , which gives a thermal power extracted from the absorber of  $75 \text{ mW cm}^{-2}$  ( $66 \text{ mW cm}^{-2}$ ). For higher laser powers, when  $\eta_{\text{rad}} = 1$ , the cooling efficiency decreases but remains positive. In this ideal case, there is no source of heating since there is no nonradiative recombination. However, the efficiency decreases with the power  $P_{\text{gen}}$  because the contacts are not sufficient to extract all the photogenerated carriers.

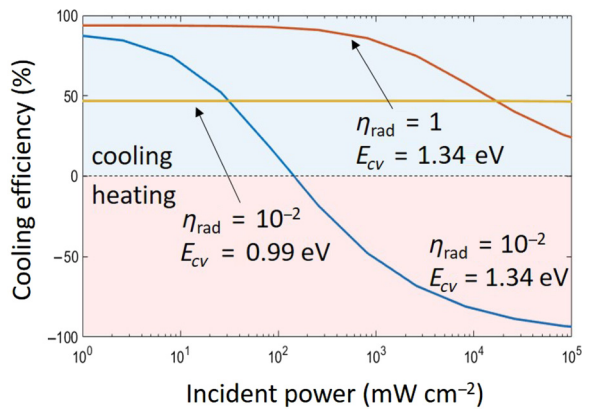


FIG. 5. Cooling efficiency  $\eta_{\text{cooling}}$  versus incident laser power considering an  $\text{In}_{0.53}\text{Ga}_{0.47}\text{As}/\text{InP}$  type-I heterojunction as shown in Fig. 4 ( $E_g = 0.74$  eV and  $E_{cv} = 1.34$  eV) with  $\eta_{\text{rad}} = 1$  and  $\eta_{\text{rad}} = 10^{-2}$ , and for a hypothetical case where  $E_{cv}$  is reduced to 0.99 eV.

There is then a significant accumulation of carriers, which implies strong radiative recombinations. We next consider a system with a single material, less efficient, where the extraction of power is done by radiative recombinations. With  $\eta_{\text{rad}} = 10^{-2}$ , the efficiency decreases as  $P_{\text{gen}}$  increases and becomes negative, corresponding to the heating of the absorber. In this case, the accumulation of carriers implies nonradiative recombinations and therefore heating. For example, for  $P_{\text{gen}} = 10^5 \text{ mW cm}^{-2}$ , the efficiency drops to  $-93\%$ . To reduce the accumulation of carriers and therefore recombinations, it would be necessary to choose a system offering a lower  $E_{cv}$ . With the same power  $P_{\text{gen}}$  and the same absorber  $\text{In}_{0.53}\text{Ga}_{0.47}\text{As}$  and  $\eta_{\text{rad}} = 10^{-2}$ , but with a reservoir such that  $E_{cv} = 0.99$  eV (the case in Fig. 2), we obtain an efficiency of 47%. As can be seen in Fig. 5, with this value of  $E_{cv}$ , the efficiency is very stable over the power range considered. The system is therefore less efficient at low power but more efficient at high power.

Next we study the influence of the  $Q$  factor on our proposal. This parameter is related to the electron-phonon scattering in the material. The empirical law, given by Eq. (2), states that the power flux exchanged between the electronic and phononic baths ( $P_{\text{phonon}}$ ) is proportional to the temperature difference between these two baths ( $T_c - T_{\text{amb}}$ ). This law comes from studies of hot-carrier solar cells based on III-V materials, but no value for other materials has yet been published. To establish the impact of  $Q$  on the operation of our device, we calculate the carrier temperature and the cooling efficiency over a wide range of  $Q$  (4 orders of magnitude). We conduct these calculations for the  $\text{In}_{0.53}\text{Ga}_{0.47}\text{As}/\text{InP}$  heterostructure ( $E_g = 0.74$  eV and  $E_{cv} = 1.34$  eV) and  $\eta_{\text{rad}} = 10^{-2}$ . As shown in Fig. 5, for such a device, the laser power ( $P_{\text{gen}}$ ) must be less than  $200 \text{ mW cm}^{-2}$  to induce a net cooling. We next consider

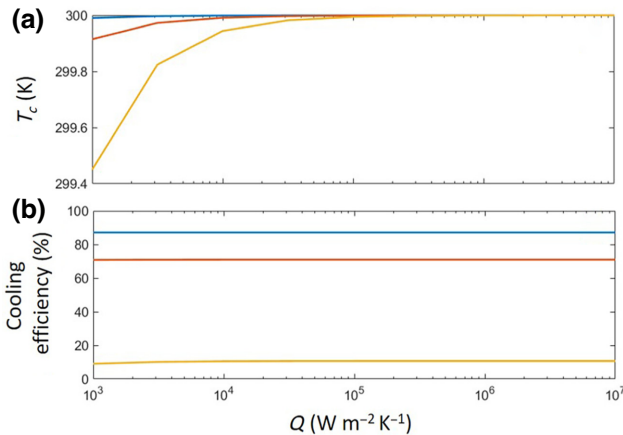


FIG. 6. (a) Carrier temperature  $T_c$  and (b) cooling efficiency  $\eta_{\text{cooling}}$  versus the electron-phonon scattering parameter  $Q$  for incident laser power of 1 mW cm<sup>-2</sup> (blue), 10 mW cm<sup>-2</sup> (red), and 100 mW cm<sup>-2</sup> (yellow).

three different laser powers: 1, 10, and 100 mW cm<sup>-2</sup>. Figure 6(a) shows the variation of  $T_c$  versus  $Q$ . Although  $T_c$  varies with  $Q$ , for the considered range of  $Q$  and for the three laser powers, we have  $\Delta T = T_c - T_{\text{amb}} < 0.6$  K. Figure 6(b) shows the corresponding cooling efficiency  $\eta_{\text{cooling}}$  versus  $Q$  for the same laser powers. Interestingly, the efficiency does not depend on  $Q$ . Indeed, for small  $\Delta T$ , the Carnot efficiency  $\eta_c$  tends to 0 [Eq. (5)] and consequently both  $P_{\text{rec}}$  and  $P_{\text{contact}}$  are almost independent of  $T_c$  [Eqs. (3) and Eq. (6), respectively]. Therefore,  $P_{\text{phonon}}$  [Eq. (7)] and  $\eta_{\text{cooling}}$  [Eq. (8)] are both principally ruled by the  $\eta_{\text{rad}}$ ,  $E_{cv}$ ,  $E_g$ , and the laser power. This last result is important because it shows that our proposal, operating at small  $\Delta T$ , is very robust and can work with a large variety of materials. Its ability to cool efficiently is governed by the design of the heterojunction, the laser power, and the ERE. The electron-phonon scattering rate, even though affecting the carrier temperature, does not influence the cooling power.

Finally, to experimentally demonstrate the cooling behavior of our device, we propose an optical characterization showing the energy up-conversion of the carriers (absorption at  $E_g$  and emission at  $E_{cv}$ ). An integrating sphere, recovering all the emitted photons, would enable us to measure the balance of the particle fluxes and the corresponding powers [23]. By measuring  $P_{\text{gen}}$ ,  $P_{\text{rec}}$ , and the power emitted by the reservoir and knowing the ERE of the absorber and the reservoir, one could deduce  $P_{\text{phonon}}$ . This characterization will be done in a future study.

#### IV. CONCLUSION

Using a detailed-balance model, we present an original cooling process in an absorber under radiation. The corresponding heat is transformed into carrier energy, which is

extracted into a large-band-gap reservoir. A large band-gap difference between the reservoir and the absorber increases the energy carried by each carrier but reduces the number of these carriers. The best trade-off, which will guide the choice of materials, depends on the desired cooling power. Compared with cooling with a single material, which requires an ERE close to 1, our proposal works even with a low ERE. Indeed, extracting heat via carrier transport rather than radiative recombination makes our system more efficient and adaptable to operating circumstances. Experimental confirmation of this process would be a major advance in heat management in semiconductor devices.

#### ACKNOWLEDGMENTS

The authors thank the Agence Nationale de la Recherche (project GELATO) for financial support (ANR-21-CE50-0017).

#### APPENDIX: DERIVATION OF $J_{\text{contact}}$ AND $P_{\text{contact}}$

Here we demonstrate the formulation of the carrier flux extracted from the left reservoir to the right reservoir ( $J_{\text{contact}}$ ), and the corresponding power flux density ( $P_{\text{contact}}$ ), in the system presented in Fig. 1. These relations are given by Eq. (6). To derive this expression, we first consider a system with selective contacts, as presented in Fig. 7.

We define  $J_L$  as the current flowing from the left reservoir to the absorber and  $J_R$  as the current flowing from the absorber to the right reservoir. These two currents are, respectively, depicted by red and blue arrows in Fig. 7. The current conservation implies that these two currents are equal; thus,

$$J_{\text{contact}} = J_L = J_R. \quad (\text{A1})$$

To express  $J_L$  and  $J_R$  we use a 3D description of the Landauer approach. Through selective contact with an energy window  $dE$ ,  $J_R$  is proportional to the difference between the electronic Fermi-Dirac distributions in the absorber and the right reservoir. Thus,

$$J_R = 2 \frac{\rho_{3D_R}}{V} v_g (f_{\text{abs}_e} - f_{\text{res}_R}) dE, \quad (\text{A2})$$

where  $\rho_{3D_R}$  is the 3D density of states in the right reservoir,  $V$  is the volume,  $v_g$  is the group velocity of the carriers, the factor of 2 accounts for spin degeneracy, and  $f_{\text{abs}_e}$  and  $f_{\text{res}_R}$  are the Fermi-Dirac distributions of electrons in the absorber and the right reservoir, respectively:

$$f_{\text{abs}_e} = \frac{1}{1 + \exp\left(\frac{E_e - \mu_e}{k_B T_c}\right)} \quad (\text{A3})$$

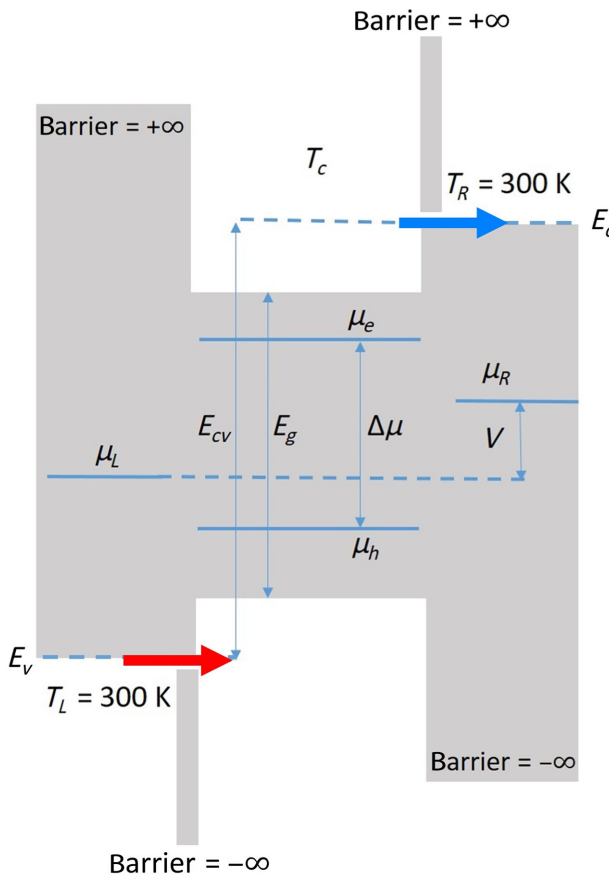


FIG. 7. The double heterojunction device with selective contacts. Electrons are injected from the right contact to the absorber with energy  $E = E_v$  (red arrow) and are extracted from the absorber to the right contact with energy  $E = E_c$  (blue arrow). The notation is identical to that in Fig. 1.

and

$$f_{\text{res}_R} = \frac{1}{1 + \exp\left(\frac{E_c - \mu_R}{k_B T_{\text{amb}}}\right)}, \quad (\text{A4})$$

where  $E_c$  is the right-contact selective energy,  $\mu_e$  and  $\mu_R$  are the electron pseudo-Fermi-levels in the absorber and the right reservoir, respectively,  $k_B$  is the Boltzmann constant, and  $T_c$  and  $T_{\text{amb}}$  are the temperature in the absorber and in the right reservoir, respectively.

Similarly,  $J_L$  is the electron current from the left contact to the absorber. For further simplification, we express  $J_L$  as the hole current from the absorber to the left contact:

$$J_L = 2 \frac{\rho_{3D_L}}{V} v_g (f_{\text{abs}_h} - f_{\text{res}_L}) dE, \quad (\text{A5})$$

where  $\rho_{3D_L}$  is the 3D density of states in the left reservoir, and  $f_{\text{abs}_h}$  and  $f_{\text{res}_L}$  are the Fermi-Dirac distributions of holes

in the absorber and the left reservoir, respectively:

$$f_{\text{abs}_h} = \frac{1}{1 + \exp\left(\frac{\mu_h - E_v}{k_B T_c}\right)} \quad (\text{A6})$$

and

$$f_{\text{res}_L} = \frac{1}{1 + \exp\left(\frac{\mu_L - E_v}{k_B T_{\text{amb}}}\right)}, \quad (\text{A7})$$

where  $E_v$  is the left-contact selective energy, and  $\mu_h$  and  $\mu_L$  are the hole pseudo-Fermi-levels in the absorber and the left reservoir, respectively. The 3D density of states in the left and right reservoirs is given by

$$\rho_{3D_L} dE = \frac{4\pi k_L^2 dk}{\frac{8\pi^3}{V}} \quad \text{and} \quad \rho_{3D_R} dE = \frac{4\pi k_R^2 dk}{\frac{8\pi^3}{V}}, \quad (\text{A8})$$

respectively, where  $k_L$  ( $k_R$ ) is the 3D wave-vector modulus in the left (right) reservoir. We describe the kinetic energy of the carriers in the conduction and valence bands using the effective-mass approximation:

$$E_{k_L} = \frac{\hbar^2 k_L^2}{2m_v^*} \quad \text{and} \quad E_{k_R} = \frac{\hbar^2 k_R^2}{2m_c^*}, \quad (\text{A9})$$

where  $E_{k_L}$  ( $E_{k_R}$ ) is the kinetic energy in the left (right) reservoir,  $\hbar$  is the reduced Planck constant, and  $m_v^*$  ( $m_c^*$ ) is the valence (conduction) effective mass in the left (right) reservoir. The group velocity  $v_g$  is given by

$$v_g = \frac{1}{\hbar} \frac{dE}{dk}. \quad (\text{A10})$$

We thus have

$$J_R = 2 \frac{1}{V} \frac{1}{2\pi^2} k_R^2 \frac{dk}{dE} \frac{1}{\hbar} \frac{dE}{dk} (f_{\text{abs}_e} - f_{\text{res}_R}) dE, \quad (\text{A11})$$

$$J_R = \frac{2m_c^* E_{k_R}}{\pi^2 \hbar^3} (f_{\text{abs}_e} - f_{\text{res}_R}) dE, \quad (\text{A12})$$

$$J_R = \frac{16\pi m_v^*}{h^3} E_{k_R} (f_{\text{abs}_e} - f_{\text{res}_R}) dE, \quad (\text{A13})$$

and

$$J_L = \frac{16\pi m_v^*}{h^3} E_{k_L} (f_{\text{abs}_h} - f_{\text{res}_L}) dE. \quad (\text{A14})$$

As  $J_{\text{contact}} = J_L = J_R$ , we have two distinct expressions for  $J_{\text{contact}}$ :

$$J_{\text{contact}} = \frac{16\pi m_c^*}{h^3} E_{k_R} \left( \frac{1}{1 + \exp\left(\frac{E_c - \mu_e}{k_B T_c}\right)} - \frac{1}{1 + \exp\left(\frac{E_c - \mu_R}{k_B T_{\text{amb}}}\right)} \right) dE, \quad (\text{A15})$$

$$J_{\text{contact}} = \frac{16\pi m_v^*}{h^3} E_{k_L} \left( \frac{1}{1 + \exp\left(\frac{\mu_h - E_v}{k_B T_c}\right)} - \frac{1}{1 + \exp\left(\frac{\mu_L - E_v}{k_B T_{\text{amb}}}\right)} \right) dE. \quad (\text{A16})$$

We introduce the notation shown in Fig. 7:  $\Delta\mu = \mu_e - \mu_h$ ,  $V = \mu_R - \mu_L$ , and  $E_{cv} = E_c - E_v$ . The kinetic energy can be expressed as  $E_{k_L} = E - E_{cv}/2$  or  $E_{k_R} = E - E_{cv}/2$ . We note that  $J_{\text{contact}}$  is proportional to the effective mass, so we consider the limiting (smallest) effective mass to go further:  $m^* = \min\{m_c^*, m_v^*\}$ . Thus,

$$J_{\text{contact}} = \frac{16\pi m^*}{h^3} \frac{(E - E_{cv})}{2} \left( \frac{1}{1 + \exp\left(\frac{E_c - \mu_e}{k_B T_c}\right)} - \frac{1}{1 + \exp\left(\frac{E_c - \mu_R}{k_B T_{\text{amb}}}\right)} \right) dE, \quad (\text{A17})$$

$$J_{\text{contact}} = \frac{16\pi m^*}{h^3} \frac{(E - E_{cv})}{2} \left( \frac{1}{1 + \exp\left(\frac{\mu_h - E_v}{k_B T_c}\right)} - \frac{1}{1 + \exp\left(\frac{\mu_L - E_v}{k_B T_{\text{amb}}}\right)} \right) dE, \quad (\text{A18})$$

which requires that

$$\frac{E_c - \mu_e}{k_B T_c} = \frac{\mu_h - E_v}{k_B T_c} \quad (\text{A19})$$

and

$$\frac{E_c - \mu_R}{k_B T_{\text{amb}}} = \frac{\mu_L - E_v}{k_B T_{\text{amb}}}, \quad (\text{A20})$$

leading to

$$J_{\text{contact}} = \frac{8\pi m^*}{h^3} (E - E_{cv}) \left( \frac{1}{1 + \exp\left(\frac{E_{cv} - \Delta\mu}{2k_B T_c}\right)} - \frac{1}{1 + \exp\left(\frac{E_{cv} - V}{2k_B T_{\text{amb}}}\right)} \right) dE. \quad (\text{A21})$$

We note that with ideal selective contacts ( $dE \rightarrow 0$  and  $E = E_{cv}$ )  $J_{\text{contact}}$  tends to zero. To consider the system shown in Fig. 1 (with semiselective contacts), we integrate Eq. (A21) from  $E_{cv}$  to  $\infty$ . Thus,

$$J_{\text{contact}} = \int_{E_{cv}}^{\infty} \frac{8\pi m^*}{h^3} (E - E_{cv}) \left( \frac{1}{1 + \exp\left(\frac{E - \Delta\mu}{2k_B T_c}\right)} - \frac{1}{1 + \exp\left(\frac{E - V}{2k_B T_{\text{amb}}}\right)} \right) dE. \quad (\text{A22})$$

The carrier temperature in the absorber  $T_c$  can be expressed with the Carnot efficiency [Eq. (5)] as  $T_c = T_{\text{amb}}/(1 - \eta_c)$ , leading to the expression given in Eq. (6). To derive the expression for  $P_{\text{contact}}$ , the corresponding power flux density, we simply note that with selective contacts,  $P = JE$ . After integration, we get the expression used in the main text.

---

Observation of laser-induced fluorescent cooling of a solid, [Nature \*\*377\*\*, 500 \(1995\)](#).

- [1] Peter Pringsheim, Zwei Bemerkungen über den Unterschied von Lumineszenz- und Temperaturstrahlung, [Z. Phys. \*\*57\*\*, 739 \(1929\)](#).
- [2] Richard I. Epstein, Melvin I. Buchwald, Bradley C. Edwards, Timothy R. Gosnell, and Carl E. Mungan, [\[3\] Jyothis Thomas, Lauro Maia, Yannick Ledemi, Younes Messaddeq, and Raman Kashyap, in \*Oxide Electronics\* \(John Wiley & Sons, Ltd, 2021\) Chap. 10, p. 353–396.](#)
- [4] Denis V. Seletskiy, Richard Epstein, and Mansoor Sheik-Bahae, Laser cooling in solids: Advances and prospects, [Rep. Prog. Phys. \*\*79\*\*, 096401 \(2016\)](#).

- [5] Manuchehr Ebrahimi, Amr S. Helmy, and Nazir P. Kherani, Plasmon coupling—the root cause of Raman anomaly and laser cooling in nanocrystal Ge, *Adv. Photon. Res.* **4**, 2200251 (2023).
- [6] Muchuan Hua and Ricardo S. Decca, Net energy upconversion processes in CdSe/CdS (core/shell) quantum dots: A possible pathway towards optical cooling, *Phys. Rev. B* **106**, 085421 (2022).
- [7] Mansoor Sheik-Bahae and Richard I. Epstein, Can Laser Light Cool Semiconductors?, *Phys. Rev. Lett.* **92**, 247403 (2004).
- [8] Jun Zhang, Dehui Li, Renjie Chen, and Qihua Xiong, Laser cooling of a semiconductor by 40 kelvin, *Nature* **493**, 504 (2013).
- [9] Son-Tung Ha, Chao Shen, Jun Zhang, and Qihua Xiong, Laser cooling of organic–inorganic lead halide perovskites, *Nat. Photon.* **10**, 115 (2016).
- [10] Daniel A. Bender, Jeffrey G. Cederberg, Chengao Wang, and Mansoor Sheik-Bahae, Development of high quantum efficiency GaAs/GaInP double heterostructures for laser cooling, *Appl. Phys. Lett.* **102**, 252102 (2013).
- [11] H. Gauck, T. H. Gfroerer, M. J. Renn, E. A. Cornell, and K. A. Bertness, External radiative quantum efficiency of 96% from a GaAs/GaInP heterostructure, *Appl. Phys. A* **64**, 143 (1997).
- [12] Guan Sun, Ruolin Chen, Yujie J. Ding, and Jacob B. Khurgin, Upconversion due to optical-phonon-assisted anti-Stokes photoluminescence in bulk GaN, *ACS Photon.* **2**, 628 (2015).
- [13] G. Rupper, N. H. Kwong, and R. Binder, Large Excitonic Enhancement of Optical Refrigeration in Semiconductors, *Phys. Rev. Lett.* **97**, 117401 (2006).
- [14] Kuan-Chen Lee and Shun-Tung Yen, Photon recycling effect on electroluminescent refrigeration, *J. Appl. Phys.* **111**, 014511 (2012).
- [15] J.-B. Wang, S. R. Johnson, D. Ding, S.-Q. Yu, and Y.-H. Zhang, Influence of photon recycling on semiconductor luminescence refrigeration, *J. Appl. Phys.* **100**, 043502 (2006).
- [16] Raphaël S. Daveau, Petru Tighineanu, Peter Lodahl, and Søren Stobbe, Optical refrigeration with coupled quantum wells, *Opt. Express* **23**, 25340 (2015).
- [17] Jacob B. Khurgin, Band gap engineering for laser cooling of semiconductors, *J. Appl. Phys.* **100**, 113116 (2006).
- [18] Nicolas Cavassilas, Imam Makhfudz, Anne-Marie Daré, Michel Lannoo, Guillaume Dangoisse, Marc Bescond, and Fabienne Michelini, Theoretical Demonstration of Hot-Carrier Operation in an Ultrathin Solar Cell, *Phys. Rev. Appl.* **17**, 064001 (2022).
- [19] Chin-Yi Tsai, Theoretical model and simulation of carrier heating with effects of nonequilibrium hot phonons in semiconductor photovoltaic devices, *Prog. Photovolt.: Res. Appl.* **26**, 808 (2018).
- [20] Maxime Giteau, Edouard de Moustier, Daniel Suchet, Hamidreza Esmaelpour, Hassanan Sodabamlu, Kentaroh Watanabe, Stéphane Collin, Jean-François Guillemoles, and Yoshitaka Okada, Identification of surface and volume hot-carrier thermalization mechanisms in ultrathin GaAs layers, *J. Appl. Phys.* **128**, 193102 (2020).
- [21] Martin A. Green, Radiative efficiency of state-of-the-art photovoltaic cells: Radiative efficiency of photovoltaic cells, *Prog. Photovolt.: Res. Appl.* **20**, 472 (2012).
- [22] Marc Bescond, Guillaume Dangoisse, Xiangyu Zhu, Chloé Salhani, and Kazuhiko Hirakawa, Comprehensive Analysis of Electron Evaporative Cooling in Double-Barrier Semiconductor Heterostructures, *Phys. Rev. Appl.* **17**, 014001 (2022).
- [23] Kazunobu Kojima, Tomomi Ohtomo, Ken-ichiro Ikemura, Yoshiaki Yamazaki, Makoto Saito, Hirotaka Ikeda, Kenji Fujito, and Shigefusa F. Chichibu, Determination of absolute value of quantum efficiency of radiation in high quality GaN single crystals using an integrating sphere, *J. Appl. Phys.* **120**, 015704 (2016).